[10] F. I. Sheftman, "Experimental study of the low frequency operation of a Cassegrainian antenna," Tech. Note 1968-38, MIT Lincoln Lab., Dec. 1968.
[11] R. Caldecott, C. A. Mentzer, L. Peters, and J. Toth, "High performance *S*-band horn antennas for radiometer use," NASA Report CR-2133, prepared by Electroscience Laboratory, Ohio State Univ., Jan. 1973.
[12] J. J. Gustincic and P. Napier, in preparation.
[13] M. H. Chen and G. N. Tsandoulas, "A wide-band square-waveguide array polarizer," *IEEE Trans. Antennas Propagat.*, vol. AP-21, pp. 389–391, May 1973.
[14] T. S. Chu and R. H. Turrin, "Depolarization properties of offset reflector antennas," *IEEE Trans. Antennas Propagat.*, vol. AP-21, pp. 339–345, May 1973.
[15] N. A. Adatia and A. W. Rudge, "Beam squint in circularly polarized offset-reflector antennas," *Electron. Lett.*, vol. 11, pp. 513–515, Oct. 1975.
[16] A. W. Rudge and N. A. Adatia, "A new class of primary-feed antennas for use with offset parabolic-reflector antennas," *Electron. Lett.*, vol. 11, pp. 597–599, Nov. 1975.
[17] P. Napier and J. J. Gustincic, in preparation.
[18] J. Kliphius and J. C. Greene, "Low noise, wideband, uncooled preamplifier," AIAA 3rd Communications Satellite Systems Conf., Paper No. 70-419, 1970.
[19] R. Clauss and E. Wieke, "Low-noise receivers: Microwave maser development," *JPL Tech. Report 32-1526*, vol. 19, pp. 95–99, Feb. 15, 1974.
[20] S. Weinreb and A. R. Kerr, "Cryogenic cooling of mixers for millimeter and centimeter wavelengths," *IEEE J. Solid-State Circuits*, vol. SC-8, pp. 58–63, Feb. 1973.

System Implications of Large Radiometric Array Antennas

CURT A. LEVIS, SENIOR MEMBER, IEEE, AND HENG-CHENG LIN, STUDENT MEMBER, IEEE

Abstract—**Current radiometric earth and atmospheric sensing systems in the centimeter wavelength range generally employ a directive antenna connected through a single terminal pair to a Dicke receiver. It is shown that this approach does not lend itself to systems with greatly increased spatial resolution. Signal-to-noise considerations relating to antenna efficiency force the introduction of active elements at the subarray level; thus if Dicke switching is to be used, it must be distributed throughout the system. Some possible approaches are suggested. The introduction of active elements at the subarray level is found to ease the design constraints on time delay elements, necessary for bandwidth, and on multiple-beam generation, required in order to achieve sufficient integration time with high resolution.**

I. Introduction

IMAGING microwave radiometers are being used increasingly to sense remotely geophysical parameters such as sea state, sea ice distribution, cloud types and distributions, and soil moisture. Instruments of this type which have evolved over the past decade differ considerably in details of design; nevertheless two basic performance parameters, viz. their angular or spatial resolution and their temperature resolution or sensitivity, have remained relatively constant over this period. This is illustrated in Table I, which compares four such systems in the range of 15–40 GHz [1]–[4]. The angular resolutions of these systems are determined primarily by the size of their antennas, which is on the order of 1 m in linear dimension for each.

TABLE I
RADIOMETER CHARACTERISTICS

	AN/AAR-33	Sea Sat-A	Nimbus E	Nimbus F
Date	1967	Proposed	1972	1975
Frequency (GHz)	15	18,22,36	19.35	37
Antenna	Paraboloids	Paraboloids	Array	Array
Beamwidth	2.2° x 1.7°	1.5° x 1.5° to 0.74° x 0.74°	1.4° x 1.4°	1.2° x 0.7°
ΔT(°K)	1.7	0.6 - 0.9	1.5	1

The payload capabilities of the Space Shuttle [5] have led to the proposal of antennas larger by an order of magnitude [6], [7], which should lead to a corresponding increase in angular resolution. The question addressed here is to what extent such antennas will be compatible with the remainder of radiometric imaging systems as they are now implemented on aircraft and satellites. It will be found that major changes in system design are required. These changes are dictated by considerations of integration time, bandwidth, and antenna losses. Of these, the antenna losses seem to have received the least attention so far, and yet they have the most far-reaching implications. Moreover, it turns out that proposed solutions for the antenna-loss problem also increase the degrees of freedom for solving the others.

II. Basic Considerations

A. General

Most current and proposed aircraft and satellite imaging radiometers are variations of the Dicke-switch type [8],

Manuscript received May 15, 1976; revised September 1, 1976. This work was supported by the National Aeronautics and Space Administration, Goddard Space Flight Center, under Contract NAS 5-20521.
C. A. Levis is with the National Center for Atmospheric Research, Boulder, CO 80303, on leave from the ElectroScience Laboratory, Department of Electrical Engineering, Ohio State University, Columbus, OH 43212.
H. C. Lin is with the ElectroScience Laboratory, Department of Electrical Engineering, Ohio State University, Columbus, OH 43212.

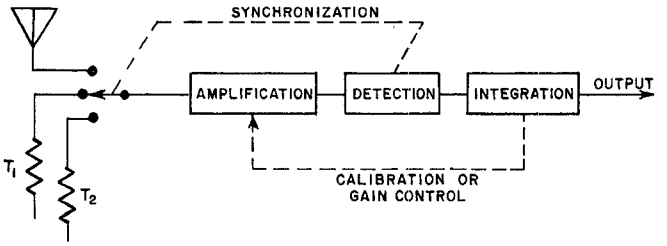

Fig. 1. Calibrated Dicke radiometric receiver.

such as that shown in Fig. 1. The limitations which arise with such a system can best be understood by referring to the basic equation for its sensitivity or temperature resolution [9], [10],

$$\Delta T = \frac{k_1 T_{\text{in}}}{\sqrt{B\tau}} \cdot S'. \tag{1}$$

In this equation, ΔT denotes the minimum detectable change of temperature at the receiver input, k_1 is a constant (typically about 2) depending on the modulation waveforms of the switching and the coherent detection reference signal, B is the predetection bandwidth, and τ is the time available for integration. S' is a system stability factor; the purpose of the second comparison load is to maintain S' near unity. The effective system input temperature is given by

$$T_{\text{in}} = 290(F - 1) + T_{\text{ant}} \quad \text{(degrees Kelvin)} \tag{2}$$

where F is the standard receiver noise figure and T_{ant} is the effective antenna temperature, given by [11], [12]

$$T_{\text{ant}} = \eta \int T_b(\Omega) f(\Omega)\, d\Omega + (1 - \eta) T_p \tag{3}$$

where η is the combined power efficiency of the antenna and the network connecting it to the receiver, $f(\Omega)$ is the antenna power pattern normalized so that its integral over all directions Ω is unity, T_b is the brightness temperature distribution observed by the antenna, and T_p is the physical temperature of the antenna and feed system.

B. Integration Time

If the spatial resolution of the array is to be maximized, the integration time in (1) must be chosen commensurate with the spatial resolution of the antenna; i.e., τ should not be larger than the time during which the combination of scanning and vehicle motion displaces the antenna beam by one beamwidth. This requirement prevents adjacent resolution elements from becoming blurred by the integration process. On the other hand, (1) shows that τ should be as large as possible, consistent with the preceding limitation, in order to minimize ΔT and thus maximize sensitivity. The integration-time dilemma is now obvious. If the antenna beamwidth is divided by n in each plane, for an aircraft or low-orbit satellite system this will require a multiplication of the transverse scan rate by n; also, n times as many resolution cells will need to be accommodated within each scan (assuming constant swath width). Thus the integration time available per resolution element will be decreased by a factor of n^2, increasing the temperature uncertainty ΔT by a factor of n according to (1). A possible way to circumvent this problem would be the use of multiple beams as indicated in Fig. 2. This approach does not turn out to be useful, however, because of the losses introduced by the beam-forming network. As will be shown in the following, the large array antenna is in quite sufficient trouble because of basic antenna losses without the addition of any further network losses between the elements and the Dicke switch.

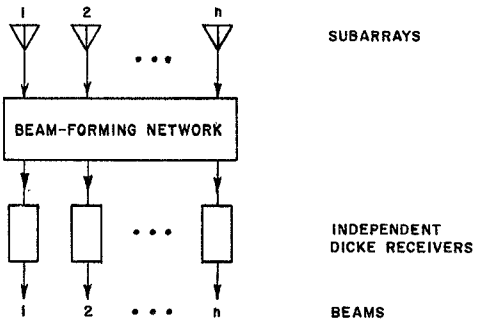

Fig. 2. Multiple-beam radiometer with radio-frequency beam forming.

C. Array Bandwidth

The frequency bandwidth of antenna arrays is well known to be inversely proportional to the maximum array dimension when the phase shifter characteristics are assumed to produce a phase shift which is independent of frequency. Thus an increase in antenna size would decrease the predetection bandwidth B and, according to (1), affect sensitivity adversely. This effect can be overcome by the use of true time delays instead of phase shifters, or, what is equivalent, of phase shifters whose phase shift at any phase shift setting is directly proportional to frequency over the bandwidth of the radiometer. Such devices are, however, not readily available in the centimeter wavelength range, especially if the requirements of good phase stability and low loss are added.

D. Antenna Losses

The effect of antenna losses seems to have received relatively less attention in the literature, yet it becomes of great importance as antenna size is increased. Before dealing with this concept quantitatively, a brief intuitive discussion may be in order. In present array technology, the elements are connected to the Dicke switch via a network of transmission lines (generally waveguides), power dividers, and phase shifters. As the array size is increased, the transmission line lengths increase and so do the number of power dividers, hence the efficiency decreases. If the array is looking at a constant brightness temperature T_b, the integral in (3) is independent of antenna pattern and becomes

$$T_{\text{ant}} = \eta T_b + (1 - \eta) T_p. \tag{4}$$

Since the first term represents the radiometric signal while the second represents internal noise, we can define a radiometric signal-to-noise ratio

$$S/N = \eta T_b / (1 - \eta) T_p \tag{5}$$

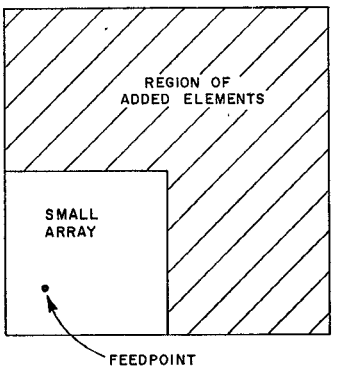

Fig. 3. Large array, considered as a smaller array with added elements.

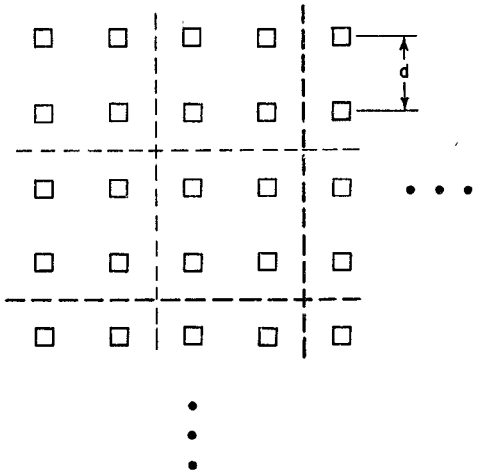

Fig. 4. Array geometry for two-dimensional corporate-fed antenna.

and a relative (temperature-independent) ratio

$$R' \equiv (S/N)/(T_b/T_p) = \eta/(1 - \eta). \quad (6)$$

From this relationship it is apparent that an increase in array size, with its accompanying decrease in efficiency, lowers the radiometric signal-to-noise ratio.

Another intuitive way of looking at the problem is to consider first a small array and then the large array that can be derived from it by the addition of more elements, as in Fig. 3. The added elements, having longer transmission paths, contribute less signal and more thermal noise relative to those of the small array. Thus, assuming the aperture illumination taper is not changed, the large array will have better spatial resolution but poorer sensitivity than the smaller array.

III. Relative Signal-To-Noise Ratio Calculations

These intuitive concepts will now be put on a firmer numerical basis. Calculations have been made for a variety of feed configurations; here we will use as an example the case of a uniformly corporate-fed antenna, with the elements arranged in groups of four at each level. The element geometry is a square grid as shown in Fig. 4. To illustrate the method of connection, the one-dimensional analog is shown in Fig. 5 in which elements are connected repeatedly in groups of two. The two-dimensional analog is not easy

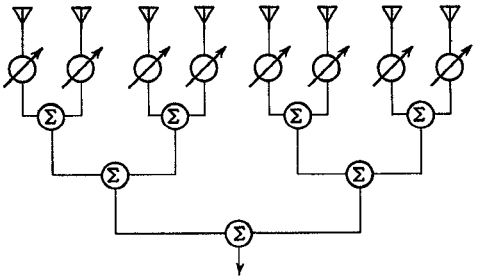

Fig. 5. One-dimensional analog for the two-dimensional corporate-fed array.

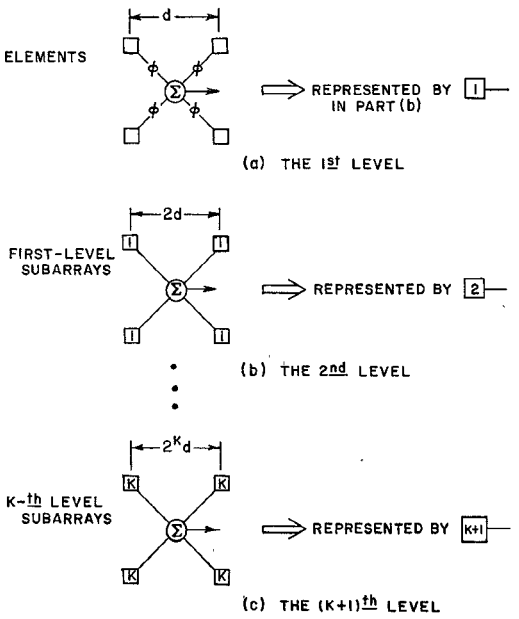

Fig. 6. Recursive scheme for generation of two-dimensional corporate-fed array.

to show on paper because the transmission line paths overlap, but the scheme is indicated in Fig. 6. Four adjacent elements are first combined into first stages (analogous to groupings of two elements in the one-dimensional case); four first-stage groups, consisting of four elements each, are combined into second-stage groups (analogous to the four-element groupings in the one-dimensional array), etc. By examining the behavior of the array as the number of stages increases, a wide range of array sizes can be examined. The number of elements is 4^r, where r is the number of stages or levels of combining.

First let us examine the signal-to-noise ratio as a function of array size when the array is used as a receiver for point-source radiation as in a communications receiver. Since the antenna is a linear device, the signal received will always be proportional to the field strength. Thus if we denote by S_0 the signal available at each element (in the presence of all other elements, i.e., with coupling effects taken into account but neglecting edge effects since the array is large), then the signal delivered to the final summation point will be proportional to S_0. On the other hand, the noise contributions due to losses in the antenna system will be proportional to kT_pB, where k is Boltzmann's constant and T_p

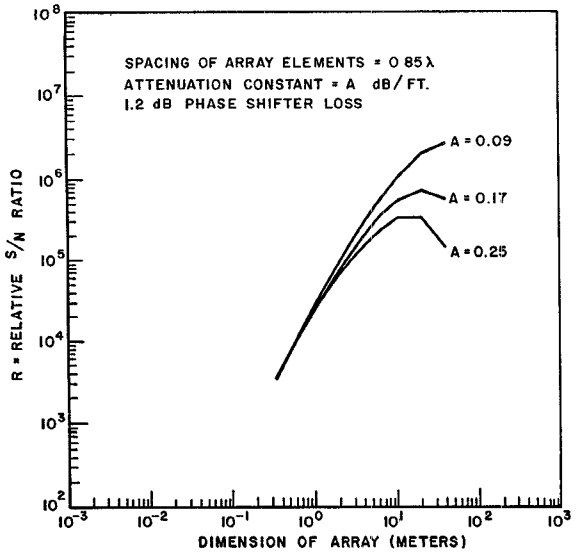

Fig. 7. Normalized signal-to-noise ratio of the corporate array for reception of a single-directional signal at 30 GHz.

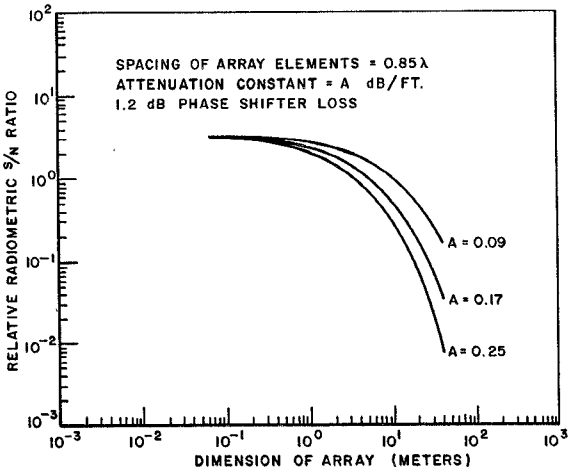

Fig. 8. Relative signal-to-noise ratio of the corporate array for reception of a spatially uniform radiometric signal at 30 GHz.

and B are the physical antenna temperature and RF bandwidth, as before. Since these quantities are not directly related to properties of the antenna, the calculations which follow deal with normalized signals s, (the actual signal divided by S_0) and normalized noise n, (the actual noise power divided by kT_pB). This yields a normalized signal-to-noise ratio R

$$R = s/n \tag{7}$$

from which the actual signal-to-noise ratio may be computed by

$$S/N = R(S_0/kT_pB). \tag{8}$$

The normalized signal can be computed for an r-level corporate-fed network by a recursive process [13]

$$s_1 = 4Te^{-2\alpha d_1}, \qquad d_1 = d/\sqrt{2} \tag{9}$$

$$s_q = 4s_{q-1}e^{-2\alpha d_q}, \qquad d_q = 2d_{q-1}, \quad q = 2,\cdots,r \tag{10}$$

and the normalized noise can be similarly computed as

$$n_1 = 1 - Te^{-2\alpha d_1} \tag{11}$$

$$n_q = 1 + (n_{q-1} - 1)e^{-2\alpha d_q}, \qquad q = 2,\cdots,r \tag{12}$$

where α is the logarithmic attenuation coefficient of the transmission lines (nepers per unit length) and T is the power transmission coefficient of the phase shifters. Loss in the power combiners has been ignored, thus producing a deliberately optimistic estimate of the normalized signal-to-noise ratio. The inclusion of loss in the power dividers is not unduly complicated [14], [15], but it merely introduces an additional parameter which has the same effect as increasing the transmission line attenuation. A plot of the normalized signal-to-noise ratio of the square corporate-fed array discussed previously, operating at 30 GHz, is shown in Fig. 7. Numerous curves for other element spacings, loss parameters, and feed configurations may be found in [13], which also lists the computer (Fortran IV) codes for their generation. All show the same characteristic shape: At a characteristic size, typically approximately 10 m on a side at 30 GHz, the signal-to-noise ratio begins to saturate and then decreases.

The preceding calculation considered the case of a spatially coherent signal, i.e., one arriving from a specific direction, as in a communications situation. In the radiometric application, the radiometric signal arrives over a range of directions, and the output temperature of the antenna is given by (3) as the convolution of the normalized antenna power pattern with the spatial brightness distribution seen by the antenna. A different output will, of course, be obtained for different brightness distributions; we shall assume here that the brightness is constant over the largest resolution element, i.e., the greatest antenna beamwidth to be considered. It would, of course, be possible to calculate the efficiency of each array configuration and obtain the signal-to-noise ratio by (6). An alternate method was used which yields the same result. It is based on the observation that for the corporate-fed arrays examined here, the beamwidth varies inversely as the linear dimension since the aperture distribution remains unchanged as elements are added by increasing the number of stages. Thus the beam area varies inversely as the number of elements m, where m is related to the number of stages or feed levels r by

$$m = 4^r. \tag{13}$$

Since contributions to the radiometric antenna temperature add in coherent fashion only from directions within the beamwidth of the antenna, the radiometric signal decreases as $1/m$, while the thermal noise contribution remains that as given by (12). As a result, a value of the relative signal-to-noise performance of the array for radiometric application can be obtained by simply dividing each value of R in Fig. 7 by the number of elements in the array m. The result is shown in Fig. 8; it is consistent with (6).

It is evident in this figure that for small numbers of elements the radiometric signal-to-noise ratio is independent of the number of elements and therefore of the beamwidth.

This well-known behavior is also evident from (6). For small arrays, the transmission line losses are small compared to those in the phase shifters, and the efficiency is relatively constant until the increased size makes the transmission line losses comparable to the phase shifter losses. Beyond this point, the radiometric signal-to-noise ratio deterioriates dramatically, and it can be seen that for 30 GHz the 1-m dimension of current radiometric arrays is near the knee of the curve. Since the Nimbus arrays are not corporate-fed structures, no precise conclusions should be drawn from this fact; yet it is suggestive of the possibility that scaling of such systems by an order of magnitude would run into serious difficulties from the standpoint of radiometric signal-to-noise ratio. This is further supported by (3) and the fact that the antenna loss for the Nimbus F radiometer is on the order of 2.8 dB, corresponding to an efficiency of about 52 percent [4].

The corporate-fed structure with uniform distribution, which has been discussed so far, is unique in preserving the same transmission line length between all elements and the feed point; both the signal and the noise from each element contribute therefore to the sum signal with equal weight, compared to any other element. This is not true of other configurations. The examination of at least one other configuration is instructive because it illustrates the tradeoffs between signal-to-noise performance (and therefore sensitivity) and angular resolution which are possible. Consider a centrally parallel-fed square array. The geometry is precisely as shown in Fig. 4. Each element is connected to the feedpoint via the shortest possible transmission path and a single phase shifter; at the feed all signals are combined in a single lossless combiner. (Such a device does not exist, but it is possible in principle and convenient for the illustration.) Suppose the designer has the choice of combining the signals from the elements with arbitrary weights. If he chooses to utilize a uniform aperture distribution, he has to assign the highest weights to the furthest elements because these have the highest transmission losses; in fact, the weights will have to be precisely inversely proportional to the transmission loss from each element. The pattern will then be that of a uniform amplitude distribution, with the corresponding good resolution, but the signal-to-noise ratio will suffer because the signals with most strongly attenuated signal and greatest thermal noise at the summing point will be emphasized. Alternatively, the designer may choose to combine the signals in an optimum S/N ratio combiner sense, i.e., with weights proportional to the signal-to-noise ratio of each input at the summing point. This would emphasize the near-in elements and greatly deemphasize the far elements; consequently, the resolution gain due to the far elements becomes marginal for large arrays. It is seen that the signal-to-noise ratio versus resolution dilemma is not limited to the corporate-fed array discussed previously, but is a general feature of large arrays. The uniformly weighted parallel arrays is discussed in more detail in [13], and computer codes for the calculations are given there.

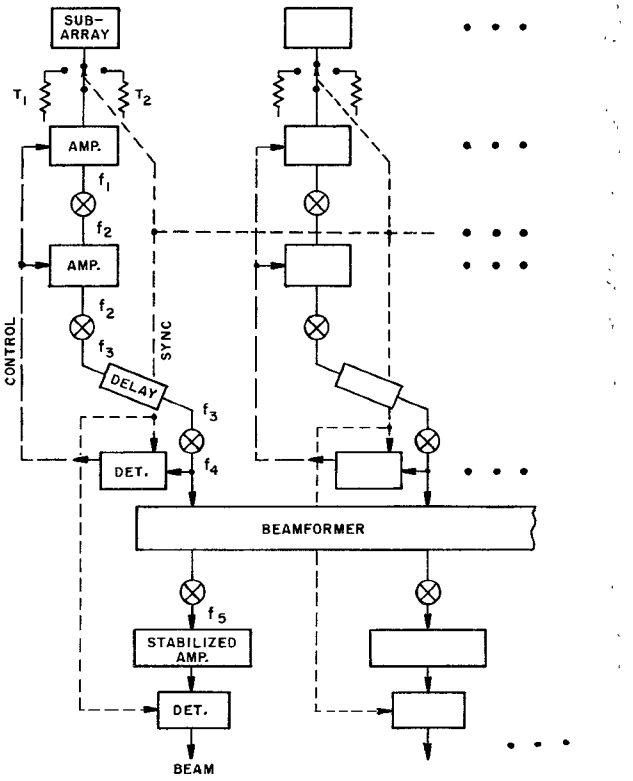

Fig. 9. Modified Dicke receiver. The switches are distributed to allow the introduction of amplification at the subarray level. The preamplifiers may be inappropriate in some frequency ranges. The frequency conversions are chosen to facilitate designing of amplifiers, delay networks, and beam former; not all indicated conversions may be necessary.

IV. Possible Solutions

From the preceding discussion it is apparent that it is not satisfactory to allow a long lossy transmission path between distant array elements and the final summing point. One method of avoiding this is to divide the array into subarrays and to introduce amplification at the subarray level. This means, however, that if Dicke switching is to be used then it must also occur at the subarray level. One possible general configuration of such a system is shown in Fig. 9. The switches are all synchronized, so that all subarrays are connected to their respective switches simultaneously. Since the signals following amplification are at a high level, the signal-to-noise ratio is established at this point and losses further down the signal path have little effect. It therefore becomes possible to convert the signal to other frequencies; for example f_2 could be chosen so as to optimize the linearity of the time delays (which could be quite lossy, e.g., acoustical devices might be used); and f_3 could be chosen to optimize the beam-forming matrix, which also could be lossy in this system. In this way the introduction of distributed Dicke switching and amplification at the subarray level would help not only in regard to maintaining radiometric signal-to-noise ratio, but it would also ease the design problems associated with bandwidth and integration time (by use of multiple beams) by allowing the use of lossy devices in optimized intermediate-frequency

ranges. There are, of course, numerous engineering problems to be resolved, e.g., the synchronization and distribution of the local oscillator signals over the structure. In truly large arrays this might be accomplished by phase-locking local sources to a master oscillator by means of modulated optical signals transmitted to the subarrays. We do not pretend to have reduced such a system to practice; we are merely suggesting it as one possible means of avoiding the basic problems which arise when the present two-terminal antenna/single Dicke-switch system is extended to much larger apertures.

Other approaches are worthy of exploration. Among these are correlation arrays [16] which are finding increasing application in radio astronomy [17]–[19]. They require extensive data processing, but in consideration of the weight capabilities of such vehicles as the Space Shuttle and the advent of microprocessors, they should not be ruled out. Most applications of such arrays in astronomy have led to their evaluation for the mapping of point sources or sources of limited extent surrounded by much larger cold regions. Their consideration for earthward sensing would seem to deserve more consideration.

V. Conclusions

The extension of present remote-sensing radiometry techniques to larger systems for higher spatial resolution is hindered primarily by antenna-loss effects which reduce temperature sensitivity. Bandwidth and integration time are also considerations which complicate the use of large antennas. The introduction of active devices at the subarray level, with consequent system modifications such as distributed Dicke switching or correlation detection, appear to merit further development if orders-of-magnitude increases in resolution are to be realized.

References

[1] *AN/AAR-33 Airborne Radiometer System.* Final Report. Sperry Rand Corporation, Clearwater, Florida, 1967. NTIS accession number AD 674 780.

[2] W. E. Scull (director) *SEASAT-A Phase A Study Report.* NASA Goddard Space Flight Center, Greenbelt, MD, pp. 3–120f, Aug. 1973.

[3] *Final Report for the Electrically Scanning Microwave Radiometer for Nimbus E.* Aerojet Electrosystems Co., Azusa, CA, Jan. 1973. Company report 1740FR-1, NASA CR-132812, NTIS accession N73-32342.

[4] *Operations and Maintenance Manual Nimbus F Electrically Scanning Microwave Radiometer.* Report 1741-OM-1, Contract NAS 5-21635. Aerojet Electrosystems Co., Azusa, CA, revised 1974.

[5] *Scientific Uses of the Space Shuttle.* Space Shuttle Board, National Research Council, National Academy of Sciences, Washington, DC, 1974.

[6] E. A. Wolff, *Shuttle Communications Experiments.* 1974. Document X-950-74-317, NASA Goddard Space Flight Center, Greenbelt, MD.

[7] L. J. Ippolito, W. H. Kummer, and C. A. Levis, "Space Shuttle millimeter wave experiment," *IEEE Intercon 75* paper E/3, 1975.

[8] R. H. Dicke, "The measurement of thermal radiation at microwave frequencies," *Review of Scientific Instruments*, vol. 17, pp. 268–275, 1946.

[9] D. F. Wait, "The sensitivity of the Dicke radiometer," *Journal of Research of the National Bureau of Standards*, vol. 71C, pp. 127–152, 1967.

[10] M. E. Tiuri in *Radio Astronomy* by J. D. Kraus. McGraw-Hill, 1966, ch 7.

[11] H. C. Ko in *Microwave Scanning Antennas*, Vol. I, R. C. Hansen, Ed. Academic Press, 1964, ch. 4, p. 277.

[12] A. E. Siegman, "Thermal noise in microwave systems. Part 1, Fundamentals," *Microwave J.*, vol. 4, pp. 81–90, Mar. 1961.

[13] H. C. Lin, *Noise Performance of Very Large Antenna Arrays.* Report 3931-1, The ElectroScience Laboratory, Ohio State University, also available as NASA-CR-144716, NTIS accession no. N76-15333/7WY, 1975.

[14] D. F. Wait, "Thermal noise from a passive linear multiport," *IEEE Trans. Microwave Theory Tech.*, vol. MTT-16, pp. 687–691, Sept. 1968.

[15] H. H. Grimm, "Noise computations in array antenna receiving systems," *Microwave J.*, vol. 6, pp. 86–90, June 1963.

[16] K. Fujimoto, "On the correlation radiometer technique," *IEEE Trans. Microwave Theory Tech.*, vol. MTT-12, pp. 203–212, 1964.

[17] M. Ryle, "Radio telescopes of large resolving power," *Reviews of Modern Physics*, vol. 47, pp. 557–566, July 1975.

[18] *The VLA: A Proposal for a Very Large Array Radio Telescope*, National Radio Astronomy Observatory, Green Bank, WV, 1967.

[19] D. S. Heeschen, "Radio astronomy: A large antenna array," *Science*, vol. 158, pp. 75–78, Oct. 6, 1967.